



## Modeling the eco-physiology of the purple mauve stinger, *Pelagia noctiluca* using Dynamic Energy Budget theory



Starrlight Augustine<sup>a,b,\*</sup>, Sara Rosa<sup>c</sup>, Sebastiaan A.L.M. Kooijman<sup>d</sup>,  
François Carlotti<sup>a,b</sup>, Jean-Christophe Poggiale<sup>a,b</sup>

<sup>a</sup> Aix Marseille Université, CNRS/INSU, IRD, Mediterranean Institute of Oceanography (MIO), UM 110, 13288 Marseille, France

<sup>b</sup> Université de Toulon, CNRS/INSU, IRD, Mediterranean Institute of Oceanography (MIO), UM 110, 83957 La Garde, France

<sup>c</sup> Department of Animal Biology and Marine Ecology, University of Messina, Viale Ferdinando Stagno D'Alcontres, 31, 98166, Messina, Italy

<sup>d</sup> Department of Theoretical Biology, Vrije Universiteit, Amsterdam, The Netherlands

### ARTICLE INFO

#### Article history:

Received 17 June 2013

Received in revised form 1 April 2014

Accepted 10 June 2014

Available online 21 June 2014

#### Keywords:

*Pelagia noctiluca*

Metabolism

Growth

Reproduction

Development

Bioenergetics

### ABSTRACT

Parameters for the standard Dynamic Energy Budget (DEB) model were estimated for the purple mauve stinger, *Pelagia noctiluca*, using literature data. Overall, the model predictions are in good agreement with data covering the full life-cycle. The parameter set we obtain suggests that *P. noctiluca* is well adapted to survive long periods of starvation since the predicted maximum reserve capacity is extremely high. Moreover we predict that the reproductive output of larger individuals is relatively insensitive to changes in food level while wet mass and length are.

Furthermore, the parameters imply that even if food were scarce (ingestion levels only 14% of the maximum for a given size) an individual would still mature and be able to reproduce. We present detailed model predictions for embryo development and discuss the developmental energetics of the species such as the fact that the metabolism of ephyrae accelerates for several days after birth. Finally we explore a number of concrete testable model predictions which will help to guide future research. The application of DEB theory to the collected data allowed us to conclude that *P. noctiluca* combines maximizing allocation to reproduction with rather extreme capabilities to survive starvation. The combination of these properties might explain why *P. noctiluca* is a rapidly growing concern to fisheries and tourism.

© 2014 Elsevier B.V. All rights reserved.

### 1. Introduction

*Pelagia noctiluca* (Forskål 1775) is a holoplanktonic cnidarian (Scyphozoa, Semaestomeae, Pelagiidae). It can form spectacular blooms which have been observed in the Mediterranean Sea (Daly Yahia et al., 2003; Ferraris et al., 2012; Goy et al., 1989; Kogošek et al., 2010; Malej, 1989a). The societal and commercial repercussions of these blooms are considerable because beaches can be closed for tourism and fishing can be negatively impacted (CIESM, 2001; Mariottini et al., 2008). This has motivated considerable research onto the biology of this species with an aim to combine individual-based models with population and physical transport models in order to predict when and where blooms are likely to occur. The present study contributes to those objectives.

From a more fundamental standpoint, *P. noctiluca* is a unique species in its own right because it does not have a polyp stage: planula undergo direct development to ephyrae (Berrill, 1949). Other species such as

*Aurelia aurita* sport facultative direct development depending on the size of the egg (Berrill, 1949; Kakinuma, 1975); hence direct development is an interesting phenomenon to study from a bioenergetic standpoint. We refer the reader to Rottini Sandrini and Avian (1983) for the definition of the above-mentioned life-stages.

A large scale scan of the literature for detailed growth and reproduction experiments for Scyphozoa in general revealed that very little quantitative numbers have been recorded even though a number of species are cultured in aquaria (Arai, 1997). *P. noctiluca* turns out to be one of the 'better studied' species. Indeed Malej and co-workers provide a rich array of laboratory and field data combined with population level modeling studies for this species (Malej, 1989a,b, 1991; Malej and Malej, 1992; Malej et al., 1993). Furthermore, detailed studies describe the process of oocyte maturation, development of planula to ephyrae and how this relates to environmental food and temperature (Avian, 1986; Avian and Rottini Sandrini, 1991; Rottini Sandrini and Avian, 1983, 1991).

Flexibility in timing and size at sexual maturity as well as the metabolic handling of starvation are key processes in *P. noctiluca* population dynamics (Malej and Malej, 1992, 2004) but they operate at the level of the individual. Hence these processes must first be assessed and

\* Corresponding author at: Aix Marseille Université, CNRS/INSU, IRD, Mediterranean Institute of Oceanography (MIO), UM 110, 13288 Marseille, France.  
E-mail address: [staug@aquadtu.dk](mailto:staug@aquadtu.dk) (S. Augustine).

understood for individuals before extrapolating to populations. Our study contributes to solving this problem. First, by quantifying those processes on the basis of what is already known (literature data) using a generic bio-energetic model and second, by working out predictions for how those processes will behave in testable situations.

We decided to use the generic bio-energetic model provided by Dynamic Energy Budget (DEB) theory: the standard DEB model (Kooijman, 2010). The idea is that the standard DEB model applies to all animals and that differences between species are captured by differences in parameter values. A brief overview of the theory is presented in Sousa et al. (2010). Recently the standard DEB model has been extended to accommodate metabolic acceleration which occurs in the early larval stages of numerous taxa (Kooijman et al., 2011; Kooijman, accepted for publication). We use the standard DEB model extended to include metabolic acceleration because, at this stage of the development of DEB theory, it is the most general model for animals; absence of acceleration becomes a special case (see Subsection 2.1).

This study was conducted in the following way. First, all published data on the eco-physiology of *P. noctiluca* are compiled; the standard DEB model with acceleration in combination with the parameter estimation technique are succinctly described. Next, parameters for the model are estimated; this amounts to quantifying investment in both reproduction and growth at varying food availability and water temperatures. The presence (or absence) of metabolic acceleration is also identified at this stage. In the third section we compare model predictions with data and present a number of testable implied model properties. The implied properties of the model are then critically evaluated in the discussion against qualitative knowledge on the species. Finally, we discuss the modular set-up of DEB theory which enables extending the DEB model to deal with starvation and more detailed reproductive physiology.

## 2. The DEB model

The way metabolism is conceptualized by the standard DEB model is presented in Fig. 1. Rectangles represent (state) variables: food, feces, reserve ( $E, J$ ), structural volume ( $V, \text{cm}^3$ ), maturity ( $E_H, J$ ) and reproduction ( $E_R, J$ ). Rounded boxes represent sinks: somatic and maturity maintenance. Arrows represent energy fluxes expressed in  $J d^{-1}$ . The model equations are listed in Table 1. Each energy flux is represented by a number in Fig. 1. The equations corresponding to each number can be found in the first part of Table 1. Below we first succinctly describe the standard DEB model extended to include metabolic acceleration. Then we define the meaning of “starvation” in the DEB modeling

framework model and specify the simple extension we adopt to cover that scenario.

### 2.1. Standard DEB model with metabolic acceleration

Briefly, energy from food is assimilated into the reserve. This constitutes the assimilation flux  $\dot{p}_A = f\{\dot{p}_{Am}\}V^{2/3}$ . The parameter  $f$ , is the scaled functional response and  $0 < f < 1$  where 0 is no food and 1 is maximum amount of food ingested for an organism of structural volume  $V$ .  $\{\dot{p}_{Am}\}$  ( $J d^{-1} \text{cm}^{-2}$ ) is the maximum surface-area specific assimilation rate and is a model parameter.  $V^{2/3}$  is the structural surface area and  $L = V^{1/3}$  is the structural length. Any type of measured length (e.g. bell diameter),  $\mathcal{L}$ , is taken proportional to  $L$  such that  $\mathcal{L} = L/\delta_{\mathcal{L}}$  where  $\delta_{\mathcal{L}}$  is the shape coefficient.

The change in reserve density,  $[E] = E/V$ , in absence of assimilation is proportional to reserve density, where the proportionality factor is the parameter energy conductance  $\dot{v}$  with dimension  $\text{cm} d^{-1}$ . A fixed fraction  $\kappa$  of the reserve mobilization flux  $\dot{p}_C$  is mobilized towards somatic maintenance and growth. The energy flux allocated to somatic maintenance,  $\dot{p}_M$  is proportional to structural volume:  $\dot{p}_M = [\dot{p}_M] V$ . Somatic maintenance comprises activity and behavior costs in addition to protein turnover. Growth,  $\dot{p}_G$ , is defined herein as the synthesis of structure; the parameter  $[E_G]$  ( $J \text{cm}^{-3}$ ) quantifies the cost of a unit of structural volume. Strong homeostasis assumptions underlying DEB theory imply that constant mass/volume to energy couplers link mass fluxes to energy fluxes. For given values of those couplers, the conversion efficiency of reserve to structure,  $\kappa_C$  is an implied model property. We present the model in a time-length-energy framework (Kooijman, 2010) in the main text to simplify presentation. How the time-length-energy framework maps to a time-length-mass framework is described in Online Appendix A.

$(1-\kappa)\dot{p}_C$  is mobilized towards maturity maintenance and maturity (before puberty) or reproduction (after puberty). The sum of the energy of  $E$  and  $V$  make up the energy fixed in the biomass of the organism. Energy invested into reproduction accumulates in what we shall call a reproduction buffer before being released into the environment in the form of gametes with efficiency  $\kappa_R$ . The energy invested in maturity, somatic and maturity maintenance as well as reproduction overheads,  $(1 - \kappa_R) dE_R / dt$ , all contribute to the dissipation flux  $\dot{p}_D$ . Maturity can be conceptualized as the cumulative amount of energy invested to reach each stage of development up till puberty, see e.g. Augustine et al. (2011a). After puberty the organism stops allocating to maturity and starts allocating to reproduction.

As a first approximation we neglect the contribution of the reproduction buffer to total biomass for *P. noctiluca* and the number of eggs

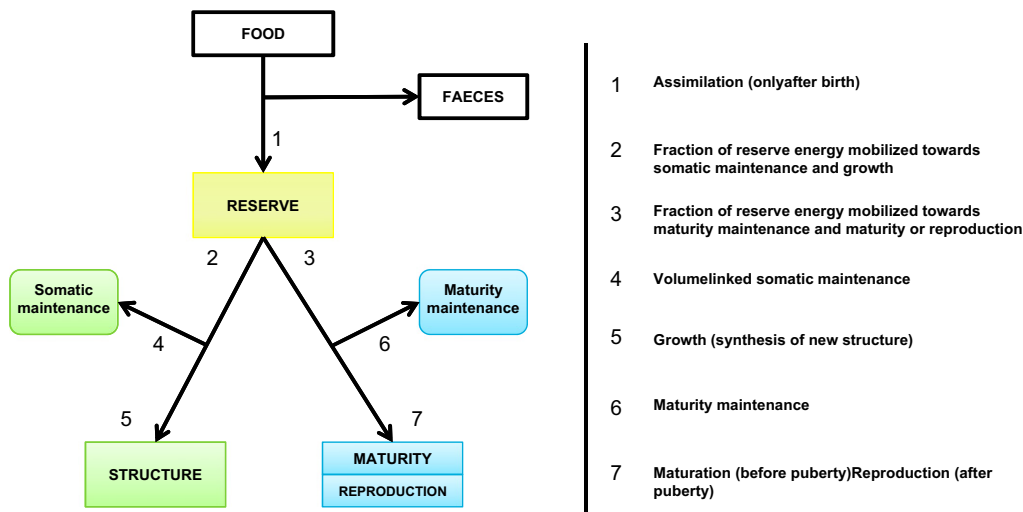


Fig. 1. Schematic view of standard DEB model. Rectangles: state variables, food and feces; arrows: energy fluxes ( $J/d$ ), rounded boxes: sinks (maintenance costs). Each energy flux is a function of primary DEB model parameters listed in Table 2 and the corresponding equations are listed in Table 1.

**Table 1**  
Equations of the standard DEB model with metabolic acceleration (length-time-energy framework). The numbers represent energy fluxes depicted in Fig. 1. The logical booleans, e.g.  $(x < y)$  are enclosed in parentheses and have value 1 if true and value 0 if false.  $s_{\mathcal{M}}$ , Eq. (1), is the shape correction function. Symbols, description, units and values are listed in Table 2. Please see the Section A.1 (Online Appendix A) for the model expressed in a length-time-mass framework. In addition, we refer to Section A.2 (Online Appendix A) for details on how excretion and respiration rates are computed. Ultimate length  $L_m$  (cm) and maximum reserve density  $[E_m]$  ( $\text{J cm}^{-3}$ ) are simple functions of parameters and can be found in Table 5.  $[E]/[E_m] = L/L_m/s_{\mathcal{M}}$  represents the no starvation boundary in the  $f, L$  state space represented in Fig. 7C.

1	$\dot{p}_A = f \{ \dot{p}_{Am} \} s_{\mathcal{M}} L^2 (E_H > E_H^p)$	Assimilation
2	$\kappa \dot{p}_C$	Mobilized reserve allocated to soma
3	$(1 - \kappa) \dot{p}_C$	Mobilized reserve allocated to maturation or reproduction
4	$\dot{p}_M = [\dot{p}_M] L^3$	Somatic maintenance
5	$\dot{p}_G = \kappa \dot{p}_C - \dot{p}_M$	Growth (synthesis of structure)
6	$\dot{p}_j = k_j E_H$	Maturity maintenance
7	$\dot{p}_R = (1 - \kappa) \dot{p}_C - \dot{p}_j$	Maturation (before puberty), reproduction (after puberty)
	$\dot{p}_D = \dot{p}_M + (1 - \kappa) \dot{p}_C (E_H < E_H^p) + ((1 - \kappa_R) \dot{p}_R + \dot{p}_j) (E_H = E_H^p)$	Dissipation
	$\dot{p}_C = E \dot{v} s_{\mathcal{M}} / (L - \bar{r})$	Reserve mobilization
	$\dot{r} = \frac{\kappa [E] \dot{v} s_{\mathcal{M}} / (L - \bar{r}) [\dot{p}_M]}{\kappa [E] + \kappa [E_C]}$	Specific growth rate when $[E]/[E_m] \geq L/L_m/s_{\mathcal{M}}$
	$\dot{r} = \frac{\kappa [E] \dot{v} s_{\mathcal{M}} / (L - \bar{r}) [\dot{p}_M]}{\kappa [E] + \kappa [E_C]}$	Specific growth rate when $[E]/[E_m] < L/L_m/s_{\mathcal{M}}$
	$dE/dt = \dot{p}_A - \dot{p}_C$	Dynamics of reserve
	$dV/dt = \dot{p}_G / [E_G]$	Dynamics of structure
	$dE_H/dt = \dot{p}_R (E_H < E_H^p)$	Dynamics of maturity
	$dE_R/dt = \kappa_R \dot{p}_R (E_H = E_H^p)$	Dynamics of reproduction
	$J_O = \eta_{OA} \dot{p}_A + \eta_{OD} \dot{p}_D + \eta_{OC} \dot{p}_G$	Dioxygen consumption
	$J_N = \eta_{NA} \dot{p}_A + \eta_{ND} \dot{p}_D + \eta_{NC} \dot{p}_G$	Ammonia excretion

produced per day becomes  $\frac{E_0}{E_0} dE_R/dt$  with  $E_0$  (J) the energy content of an egg. According to the maternal effect implemented into the standard DEB model  $E_0$  is such that  $[E]$  of the neonate at birth equals  $[E]$  of the mother at the moment of spawning (Kooijman, 2009).

In summary, the model covers the full life-cycle of an individual and assumes iso-morphy, i.e. the ratio between surface area and volume remains constant during ontogeny (Kooijman, 2010). Birth is defined as the moment during which the assimilation of food into reserve starts

**Table 2**  
Variables and parameters of the standard DEB model. Rates are expressed reference temperature  $T_{ref}$ . Parameters  $\{ \dot{p}_{Am} \}$  and  $\dot{v}$  have two values: embryo/adult (see text). Indices O and N represent molecules of  $\text{O}_2$  and  $\text{NH}_3$  respectively. The indices A, D, and G represent assimilation, dissipation and growth powers ( $\text{J d}^{-1}$ ) respectively; please see Table 1 for model equations as well as Online Appendix A (Eq. (A.3)) for values of  $\eta_{1+2}$ .

Symbol	Value	Unit	Description
<i>Forcing variables</i>			
$f$		–	Scaled functional response ( $0 \leq f \leq 1$ )
$T$		K	Temperature
<i>State variables</i>			
$V$		$\text{cm}^3$	Structural volume
$L$		cm	Structural length $V^{1/3}$
$E$		J	Reserve
$E_H$		J	Cum. energy invested in maturation
$E_R$		J	Cum. energy invested in reproduction
<i>Dioxygen and ammonia fluxes</i>			
$J_O$		$\text{Mol O}_2 \text{ d}^{-1}$	Dioxygen consumption
$J_N$		$\text{Mol NH}_3 \text{ d}^{-1}$	Ammonia excretion
$\eta_{1+2}$		$\text{Mol}^* \text{1 J}^{-1}$ of power *2	*1 $\in [O, N]$ and *2 $\in [A, D, G]$
<i>DEB model parameters</i>			
$\{ \dot{p}_{Am} \}$	24.38/74.55	$\text{J d}^{-1} \text{ cm}^{-2}$	Maximum surface-area specific assimilation rate
$\kappa_X$	0.8 <sup>a</sup>	–	Digestion efficiency
$\kappa_X^p$	0.1 <sup>a</sup>	–	Faecating efficiency
$\kappa_R$	0.95 <sup>a</sup>	–	Reproduction efficiency
$\kappa$	0.37	–	Allocation fraction to soma
$[\dot{p}_M]$	164	$\text{J d}^{-1} \text{ cm}^{-3}$	Volume linked somatic maintenance costs
$[E_G]$	263	$\text{J cm}^{-3}$	Cost of synthesis of a unit of structure
$k_j$	0.002	$\text{d}^{-1}$	Maturity maintenance rate coefficient
$\dot{v}$	0.018/0.055	$\text{cm d}^{-1}$	Energy conductance
$E_H^p$	0.0023	J	Cum. energy investment in maturation at birth
$E_H^i$	0.073	J	Cum. energy investment in maturation at metamorphosis
$E_H^p$	1864	J	Cum. energy investment in maturation at puberty
<i>Temperature parameters</i>			
$T_A$	11270	K	Arrhenius temperature
$T_{ref}$	293	K	Reference temperature
<i>Parameters which map data to state variables</i>			
$\delta_{\mathcal{M}1}$	0.13	–	Shape coefficient for lengths for all data except Morand et al. (1987)
$\delta_{\mathcal{M}2}$	0.07	–	Shape coefficient for lengths from Morand et al. (1987)
$\delta_V$	1.98	–	Shape coefficient for yolk

<sup>a</sup> Denotes values which were fixed.

( $E_H = E_H^b$ ), while puberty is defined as a metabolic switching point where energy allocation to maturity stops and allocation to reproduction starts:  $E_H = E_H^p$ . The term sexual maturity is synonymous to puberty in this framework. The standard DEB model extended to include metabolic acceleration assumes a third important life-history event called metamorphosis where  $E_H = E_H^j$  and  $E_H^b < E_H^j < E_H^p$ . The three maturity levels  $E_H^b, E_H^j$  and  $E_H^p$  are model parameters. Metabolic acceleration occurs between birth and metamorphosis; in terms of the model this means that  $V^{2/3}$  increases proportionally to  $V$  (Kooijman et al., 2011; Kooijman, accepted for publication). Consequently both parameters with surface-area in their dimensions,  $\dot{p}_A$  and  $\dot{p}_M$ , are no longer constant but are functions of structural length:

$$s_{\mathcal{M}} = \max(L_b, \min(L, L_j)) / L_b \quad (1)$$

where  $L_b$  and  $L_j$  are the structural lengths at birth and metamorphosis respectively and  $s_{\mathcal{M}}$  is the acceleration factor. No metabolic acceleration reduces to the special case:  $E_H^j = E_H^b$ . From metamorphosis onwards the acceleration factor becomes  $s_{\mathcal{M}} = L_j / L_b$ . The value of  $L_j$  depends on the food level experienced by the individual prior to metamorphosis thus the final acceleration factor is a food dependent statistic.

Dioxygen consumption and ammonia excretion are taken as a weighted sum of assimilation, dissipation and growth fluxes ( $\dot{p}_A, \dot{p}_D$  and  $\dot{p}_G$ ); please refer to Tables 1 and 2 (and the Online Appendix A) for the full model specification.

### 2.2. Standard DEB model extended to include starvation

“Starvation” occurs when energy mobilized from reserve no longer suffices to cover somatic maintenance:  $\kappa \dot{p}_C < [\dot{p}_M] L^3$ . In the same way, maturity maintenance is no longer covered if  $(1-\kappa) \dot{p}_C < \dot{k}_j E_H$ . In our opinion, what happens should either of these situations occur must be specified else model simulations become inconsistent as soon as we start working with low food levels and any type of shrinking occurs. Augustine et al. (2011b) worked out a simple extension of the standard DEB model which covers both situations. The idea is as follows.

Briefly, if  $\kappa \dot{p}_C < [\dot{p}_M] L^3$  then (part of structure) is degraded to cover somatic maintenance with a certain conversion efficiency. To remove a parameter we take this conversion efficiency equal to  $\kappa_C$ . If structure shrinks too much the organism dies. In addition, if  $(1-\kappa) \dot{p}_C < \dot{k}_j E_H$  then it is possible for maturity level to decay and an extra parameter  $\dot{k}'_j$  is needed to quantify that decay. From a physiological standpoint, a

decay in maturity level can mean going backwards in development as has been observed for *Turritopsis nutricula* (Piraino et al., 1996) or *A. aurita* (Hammer and Jenssen, 1974) – backwards meaning free-living medusa stage to polyp. *T. nutricula* can go all the way backwards while *A. aurita* can go backwards till just before the ephyra stage but no further. Physiological repercussions of a decay in maturity level are species specific and fall outside of the scope of this study. Nonetheless the question, why would one pay maturity maintenance if going backwards in development is just as easy as going forwards, immediately jumps to mind. The idea put forth in Augustine et al. (2011b) is that there is a hazard associated with going backwards in development. The survival probability is proportional to that hazard.

For the purpose of our study, we set  $\dot{k}'_j = 0$  (so no decay in maturity level) and do not model hazard, survival probability or death by shrinking.

### 3. Methods

The data compilation and parameter estimation methods are presented in the first two subsections followed by how the goodness of fit of the model is evaluated.

#### 3.1. Data

Data on life history, growth and respiration were collected from the literature. Data points extracted from literature studies were digitalized using PlotReader (<http://jornbr.home.xs4all.nl/plotreader/>, Jorn Bruggeman). We calculate the maximum possible wet mass using allometric coefficients given in Rosa et al. (2012). Compiled data is summed up in Table 3.

In addition, we included the results from a new reproduction experiment. Sampling collection methods are described in Rosa et al. (2012). All of the sampling took place throughout the year in the Straits of Messina.

After collection from the field, medusa bell diameter was measured with a ruler and sex identified by visual observation of the gonads. During each season, couples of mature specimens were then selected and placed for 24 h in 5-liter tanks containing seawater at different temperatures (14, 17, 20 and 23 °C) using thermostatic cells. Fertilized eggs released were counted and the relation between female bell diameter and number of eggs was established.

The total number of couples was 23 however, mature females with many mature eggs were more abundant during winter (14 °C), thus

**Table 3**

Goodness of fit of model to data. Each zero- and uni-variate data set used for estimating parameters are listed here. The relative error (RE), Eq. (4), between model and each data set is presented in addition to the overall error and the goodness-of-fit mark Eq. (5). Auxiliary parameters comprising part of the mapping functions used to link DEB model state variables to measured quantities are listed under the column assumptions. Please refer to Section A.3, Online Appendix A, for more details.

Dataset	Unit	Description	RE	Assumptions	Location
Lw0	mm	Egg diameter	0	$f = 1, \delta_Y$	Table 4
Lwb	mm	Length at birth	0.1	$f = 1, \delta_{M1}$	Table 4
Lwp	cm	Length at puberty	0.2	$f = 1, \delta_{M1}$	Table 4
ap	d	Age at puberty	0.6	$f = 1, 20 \text{ }^\circ\text{C}$	Table 4,
Lm	cm	Ultimate length	0.1	$f = 1, \delta_{M1}$	Table 4
Wwi	g	Ultimate wet mass	0.2	$f = 1$	Table 4
RQ	mol/mol	Respiratory quotient	0.1	$f = 1$	Table 4
T-ab	°C – d	Temperature – age at birth	0.1	$f = 1$	Fig. 2
L-R_T	mm – # eggs/d – °C	Bell diameter - reproduction rate – different temperatures	0.3	$f = 1, \delta_{M1}$	Fig. 3
L-Ww	mm – mg	Bell diameter – wet mass	0.3	$f = 1, \delta_{M1}$	Fig. 7A
L-WC	mm – mg	Lappet to lappet length – carbon mass	0.2	$f = 1, \delta_{M2}$	Fig. 4A
L-WN	mm – mg	Lappet to lappet length – carbon mass	0.1	$f = 1, \delta_{M2}$	Fig. 4B
t-WwA	d – mg	Time – wet mass individual A	0.10	$f = 0.49$	Fig. 5
t-WwB	d – mg	Time – wet mass individual B	0.10	$f = 0.44$	Fig. 5
t-WwC	d – mg	Time – wet mass individual C	0.10	$f = 0.48$	Fig. 5
T-JO	°C – mol O <sub>2</sub> g <sup>-1</sup> dry mass	Temperature – mass specific dioxygen consumption	1.36	$f = 1$ ; dry mass 1.1 g	Fig. 4C
T-JN	°C – mol NH <sub>3</sub> g <sup>-1</sup> dry mass	Temperature – mass specific ammonia excretion	0.43	$f = 1$ ; dry mass 1.1 g	Fig. 4D
Mean relative error of all data sets:			0.25		
Goodness-of-fit:			7.5		

more specimens were collected during these months. During spring (17 °C), females had discolored and empty gonads, and appeared to have just finished spawning. Whereas in summer–autumn (20 °C and 23 °C) only medium-sized females (with less mature eggs) were mature. Thus, the number of samples available for the experiments changed with seasons (see Fig. 3).

### 3.2. The “covariation method” of parameter estimation

We use freely downloadable software DEBtool (Kooijman et al., 2008); see Table A.2 in Online Appendix A. Parameter estimates are based on the simultaneous minimization of squared deviations between a number of data sets and model predictions in a one step procedure: the “covariation method” for estimating parameters (Lika et al., 2011a,b). We use the Nelder Mead simplex method implemented in DEBtool routine ‘nmgr’.

The weighted least square (WLS) criterion applied for the covariation method of parameter estimation leads to the minimization of

$$\sum_j \sum_i \beta_{ij} (Y_{ij} - \hat{Y}_{ij})^2 \quad (2)$$

for all of the datasets simultaneously, where  $i$  corresponds to values within a data set and  $j$  scans across data sets,  $\beta_{ij}$  are weight coefficients,  $Y_{ij}$  and  $\hat{Y}_{ij}$  are observations and model predictions respectively. The weight coefficients normalize the data sets to remove effects of units and in practice are taken inversely proportional to the mean of the observations in a data set,  $\beta_{ij} = \alpha/Y_{ij}^2$ , where  $\alpha$  controls the relative weight of each data set to the total WLS function and  $Y_{ij}$  is the mean value.

Single data points (such as maximum reproduction rate, egg diameter, or length at birth) can also be used for estimating parameters and are called zero-variate data. Data sets which include an independent variable (e.g. length or time) and a dependent variable (e.g. length or developmental stage) are hereafter referred to as uni-variate data. Parameter estimation is guided by prior knowledge of parameter values implemented in the form of data; this data is hereafter referred to as pseudo-data. (Lika et al., 2011a; Saraiva et al., 2011). Zero- and uni-variate as well as real- and pseudo data are collected in Table 4.

Food and temperature are treated as forcing variables. Temperature affects time (rates, ages). We assume a simple Arrhenius relationship, Eq. (1.2) p. 17 (Kooijman, 2010):

$$k(T) = k_{\text{ref}} \exp\left(\frac{T_A}{T_{\text{ref}}} - \frac{T_A}{T}\right) \quad (3)$$

where  $k$  is a rate. We assumed a reference temperature  $T_{\text{ref}}$  of 193 K (20 °C) for comparison purposes between data sets and between

species in future studies since it is the reference temperature used in Kooijman et al. (2008), Lika et al. (2011a,b), Kooijman (2013).

We compute the mean food level for the different experiments using the scaled functional response  $f$  (see Subsection 2.1). This parameter is in fact the ratio of the actual ingestion over the maximum possible ingestion for an individual of that size which is why it can be interpreted as a mean food level for a given data set.

In this study we estimated the DEB model parameters (Table 2) from literature data (Table 3) in one step. We assumed that  $\kappa_R = 0.95$  on the basis that hardly any energy loss occurs when converting reserve material to gametes. In addition, we assumed assimilation and fecation efficiencies ( $\kappa_X$  and  $\kappa_X^p$ ) of 0.8 and 0.1 respectively.

The data we used from the literature originated from studies, in which different types of length measurements were used. The value of  $\delta_{\mathcal{M}}$  will be different between the different types of length measurements which were used: i.e. rhopalia to rhopalia, lappet to lappet, and bell diameter. Functions used to map the other observed quantities such as egg diameter, mass, dioxygen consumption, or ammonia excretion to state variables are presented in Section A.2 of the Online Appendix A since those functions use mass/volume/energy couplers needed to work in a length-time-mass framework (Table A.1, Online Appendix A).

### 3.3. Evaluation of model performance

Goodness of fit is evaluated by examining the relative error between model and data. The chemical, physical and biological “realism” of the parameter set (Lika et al., 2011a) takes precedence over goodness of fit if parameter values with a poorer fit are more realistic. Assessments of realism are provided in the form of an exhaustive list of about 100 implied model properties. The relative error (RE) of a dataset containing  $n$  data points is:

$$RE = \frac{1}{n} \sum_{i=1}^n \left| 1 - \frac{\hat{Y}_i}{Y_i} \right| \quad (4)$$

The overall error (E) is defined as the mean of all the relative errors; the goodness-of-fit of model to all data is written as:

$$FIT = 10 (1 - E) \quad (5)$$

where  $FIT \in (-\infty, 10]$ .

## 4. Results

Using the co-variation method of parameter estimation we were able to estimate DEB model parameters applicable to the full life-cycle of *P. noctiluca*. The in-depth data compilation reveals that this species

**Table 4**  
Observed and predicted values for zero-variate data. Computations are performed using  $f = 1$  and  $T = 20$  °C. Fig. 6 gives an overview of the flexibility of  $\mathcal{S}_p$  and  $a_p$  at different scaled functional responses and temperatures.

Symbol	Observed	Predicted	Unit	Description	Source
<i>Zero-variate observations</i>					
$\mathcal{S}_0$	0.25–0.3	0.3	mm	Egg diameter	Berrill (1949), Avian and Rottini Sandrini (1991), Rosa et al.(2012)
$\mathcal{S}_b$	1.1	1.2	mm	Length at birth (diameter between opposite rhopalia)	Avian (1986)
$\mathcal{S}_p$	3–4.5	5.5	cm	Length at puberty	Avian (1986)
$a_p$	150	57	d	Age at puberty	Malej and Malej (2004)
$\mathcal{S}_m$	12–14	13	cm	Ultimate length	Goy et al. (1989), Rosa et al. (2012)
$W_{wi}$	288	342	g	Ultimate wet mass	Rosa et al. (2012)
RQ	0.8	0.9	mol/mol	Respiratory quotient	Larson (1987b)
<i>Zero-variate pseudo-data</i>					
$\dot{v}$	0.020	0.02	cm d <sup>-1</sup>	Energy conductance	Lika et al. (2011a)
$\kappa$	0.80	0.37	–	Allocation fraction to soma	Lika et al. (2011a)
$\kappa_R$	0.95	0.95	–	Reproduction efficiency	Lika et al. (2011a)
$[\dot{p}_M]$	18	164	J cm <sup>-3</sup> d <sup>-1</sup>	Volume-linked somatic maintenance costs	Lika et al. (2011a)
$k_j$	0.002	0.002	d <sup>-1</sup>	Maturity maintenance rate coefficient	Lika et al. (2011a)
$\kappa_G$	0.80	0.80	–	Growth efficiency	Lika et al. (2011a)

has a data completeness level of 2 (out of 10) according to criteria from (Lika et al. (2011a), Table 3, p. 275). We fit the model to 24 data sets, 7 of which are pseudo-data, which leaves a total of 17 empirical data sets. A total of 16 parameters were estimated from the data. Predictions for zero- and uni-variate data are collected in Table 4 and Figs. 2A, 3, 4, 5 and 7A. In the following subsections we show that this parameter set makes chemical, biological and physical sense and generally matches empirical observations quite well. A subset of implied model properties are listed in Table 5. Simulation studies are presented in Figs. 2B, 6, 7B, C, 8 and 9.

#### 4.1. Comparing model predictions with available data

There is more information about embryos than juveniles (i.e. ephyrae, immature medusae) or adults. The model predicts that an egg from a well fed mother contains 0.06 J or 3  $\mu\text{g}$  ash free dry mass (Table 5). Assuming the same proportionality factor between structure and ephyra length as for adults in Rosa et al. (2012), the length at birth is close to that observed (Table 4). We compared observed and predicted ages at which the ephyra stage was reached at four separate temperatures in the study by Rosa et al. (2012), Fig. 2A. This corresponds to stage IX described in Rottini Sandrini and Avian (1983). According to Rosa et al. (2012) the embryo reaches the ephyra stage at 3 days post fertilization at 20 °C and 4 days post fertilization at 17 °C. This is in slight contradiction to Rottini Sandrini and Avian (1983) who describe the completion of ephyra development in 3.8 days at 19 °C. On the other hand Avian (1986) reports that it takes 7 days to reach the ephyra stage at 13.5 °C which is in line with model predictions. Overall the results from Avian (1986), Rosa et al. (2012) and Rottini Sandrini and Avian (1983) are coherent but show some scatter which cannot be captured by a simple Arrhenius relationship. The relative error between the model and observations is 0.1 (Table 3).

Model predictions for reproduction rate against length at 14 and 17 °C are in agreement with the data while notable deviations between model predictions and data occur at 20 and 23 °C (Fig. 3). However there are hardly any replicates at these higher temperatures which hampers firm conclusions. To our knowledge this is the only published reproduction rate against length data for *P. noctiluca* which motivates presenting it here. The reproduction rate data at 17 °C suggest that maximum reproduction rates at that temperature might reach 45,000 eggs/d. However, the model predicts a maximum reproduction rate of 24,690 eggs/d ( $f = 1$ , 20 °C, Table 5). In the future when more observations on reproduction rates are available, parameters can be re-adjusted according to new insight.

Bell diameter against mass curves are well captured by the model (Figs. 4A,B and 7A). The predictions for dry mass from Morand et al. (1987) and Rosa et al. (2012) also fit the data well when assuming a dry mass to ash free dry mass ratio of 3.6 (not shown).

There are no growth curves except for the 14 d wet mass against time data (for several adults) from Larson (1987a). We are able to fit the model to the growth of three individuals from his study by assuming a scaled functional response a little under 0.5 (Fig. 5). Predictions for dioxygen consumption for a 1.1 g (dry mass) individual are divided by that mass and computed for a range of temperatures and compared to empirical data from Malej (1989b). The high scatter will hamper arriving at any type of low relative error however we can see that model predictions are in the ball park of what has been observed (Fig. 4C,D). The goodness-of-fit mark of the model to data is 7.5 (Table 3), see Eq. (5).

#### 4.2. Implied properties/testable model predictions

We can now use the model to infer on the developmental energetics of *P. noctiluca*. Using parameters in Table 2 it is possible to compute cumulated energy invested in maturity against age during embryo development (Fig. 2B). In such a manner we can compute the energy investment to reach developmental stages I to IX described in Rottini Sandrini and Avian (1983). The model predicts that the fraction of reserve left at birth relative to the initial amount of reserve in the egg is 0.9 (Table 5). We found that we needed metabolic acceleration to capture embryo and adult metabolism with a single parameter set. Our results suggest that embryo metabolism accelerates about threefold between birth and metamorphosis.

Predictions for ultimate wet mass, length at puberty and respiratory quotient are also in good agreement with what is known about this species (Table 4). The predicted age at puberty is almost 2 months instead of the observed 6 months. It is important to realize that predictions for zero-variate data assume  $f = 1$  and 20 °C. We compute predicted length and age at puberty over a range of temperatures and scaled functional responses (Fig. 6A–C) and the observed 6 months falls within the scope of those predictions.

We always assumed constant food density, so constant  $f$ . Under this condition, the reserve density reaches an equilibrium with its environment such that  $d[E]/dt = 0$  (Kooijman, 2010, Chap. 2). The biological implication is that for each value of  $f$  there is a corresponding fixed value of  $\delta_E$ , i.e. fraction of biomass which is reserve. Furthermore, for every size there is a particular value of  $f$  such that  $\kappa \dot{p}_C = [\dot{p}_M] L^3$ . Below that value the organism begins to starve and above that value growth occurs. We plot the no growth condition for  $\mathcal{L}$  and  $f$  in Fig. 7C. There is a maximum and a minimum value of  $\delta_E$  for each size

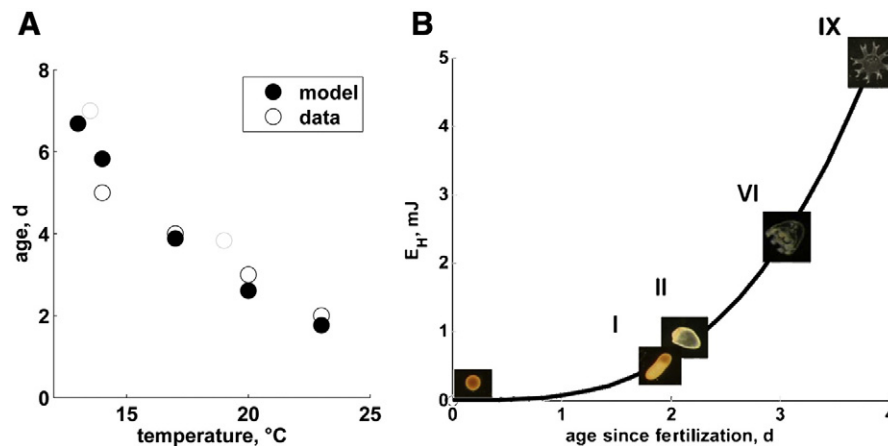


**Fig. 2.** (A) Age since fertilization (day) at which the ephyra stage is reached at different temperatures. This supplementary data is from Rosa et al. (2012). Empty symbols: data; full symbols: model predictions. The model predictions assume the maternal effect and  $f = 1$  for the mother at spawning. Empty gray circles: Avian (1986) (13.5 °C) and Rottini Sandrini and Avian (1983) (19 °C). (B) Predicted cumulative energy invested in maturity ( $E_H$ ) to reach developmental stages I, II, VI and IX as described in Rottini Sandrini and Avian (1983).  $T = 19$  °C.

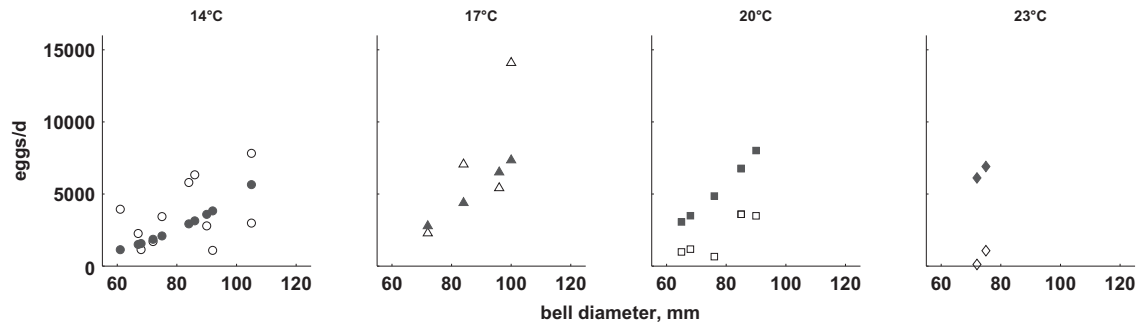


Fig. 3. Reproduction rate against length at four different temperatures. Source: this study. Empty symbols: data; full symbols: model predictions. Model predictions assume  $f = 1$ ,  $\delta_{\text{re}} = 0.13$ .

and for each value of  $f$  such that no shrinking occurs. This gives a natural prediction for the variability observed in empirical length–mass relationships: Fig. 7B.  $\delta_E$  reaches a maximum value of 0.99 for the largest size at  $f = 1$  (Table 5).

#### 4.3. Impact of changes in feeding conditions on growth and reproduction

We performed simulation studies to assess the impact of a change in feeding conditions on growth and reproduction simultaneously. To this end, predictions for two types of growth and reproduction experiments are plotted: they start at birth and continue till after puberty (Fig. 8) assuming 20 °C. In the first theoretical experiment  $f = 1$  till 18 d since birth then  $f = 1$ ,  $f = 0.5$  and  $f = 0.3$  (Fig. 8A–C). No shrinking occurs in any of the conditions. However, growth, age at onset of reproduction and the slope of cumulative reproductive output differ considerably between conditions.

In the second theoretical experiment (Fig. 8D–F) we assume  $f = 1$  till 100 d since birth,  $\approx 8$  cm bell diameter, and then drop the food level to  $f = 0.3$ . The results are now very different: wet mass and length shrink and it takes about 25 days to observe any difference in the reproductive output. Why the shrinking occurs in this second experiment at  $f = 0.3$  but not in the first experiments is explained graphically in Fig. 7B. The large maximum reserve capacity [ $E_m$ ] =  $14.0 \text{ kJ cm}^{-3}$  (Table 5) in combination with a low value of  $\kappa$  is responsible for the insensitivity of reproductive output to variations in environmental food for larger individuals.

#### 4.4. Effects of the choice of measurement on the variability and dynamics of observed respiration rates

In a final simulation experiment, we plot the predicted wet mass, reproductive output and dioxygen consumption of individual A from Larson (1987a) assuming 14 d growth at  $f = 0.46$  followed

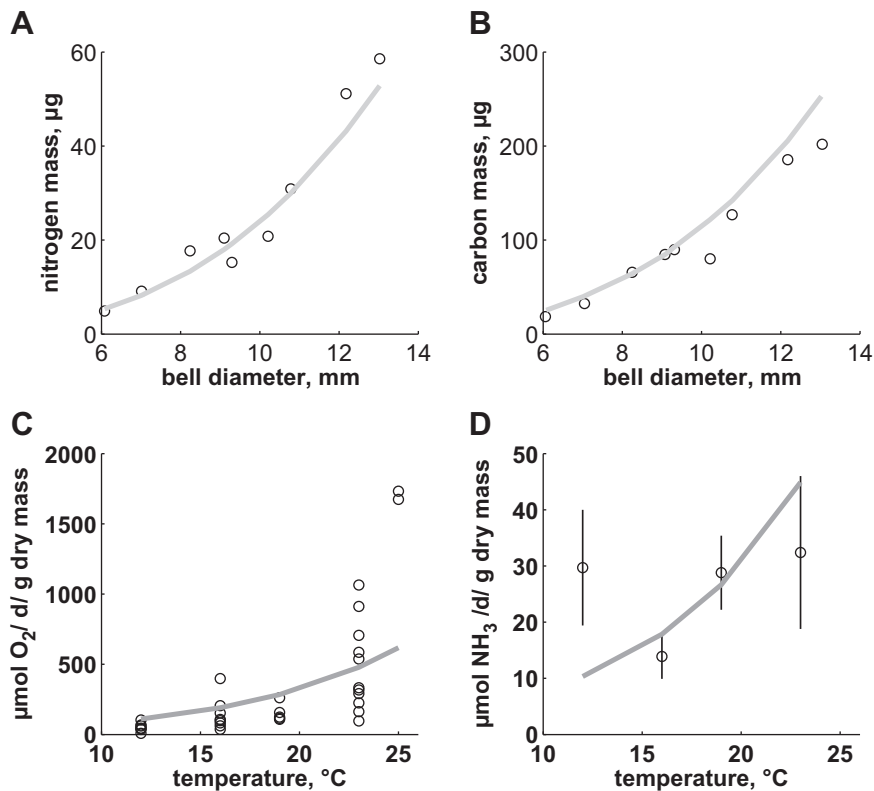


Fig. 4. Nitrogen mass (A) and carbon mass (B) against length. Source: Morand et al. (1987). Solid gray line assumes  $f = 1$  and no contribution from the reproduction buffer. See Online Appendix A for the equations. Next on the bottom row we have the mass specific dioxygen consumption (C) and ammonia excretion (D) against temperature. Source: Malej (1989b). Points in (C) were digitalized from Fig. 1 of the study while for (D) mean (circle) and standard deviation (black vertical lines) are from Table 1 of that study. Solid gray line assumes  $f = 1$ , and a dry mass of 1.1 g.

by 6 d at  $f = 0$ , Fig. 9A–B. We discuss the predicted growth and reproduction later, however what we illustrate here is that predicted dioxygen consumption expressed as  $\mu\text{mol d}^{-1}$  decreases during starvation (Fig. 9C) which is realistic. The reason is that both reserve mobilization and structure decrease during shrinking. Dioxygen consumption is actually commonly represented in three other ways in the literature:  $\mu\text{mol d}^{-1}$  against length,  $\mu\text{mol d}^{-1}$  against wet mass and as  $\mu\text{mol per gram (dry) biomass}$  as in Malej (1989b). We plot the predictions for each of these representations for that individual (Fig. 9D–F). The resulting relationships are harder and harder to interpret – this is because there is no “easy” interpretation for wet mass since it is composed of compounds pertaining to reserve and/or structure while an organism only pays somatic maintenance for its structural components. The range of predicted mass specific respiration is about 500 to 1500  $\mu\text{mol per gram (dry) biomass}$  (Fig. 9F) which is consistent with that reported in Malej (1989b).

## 5. Discussion

The standard DEB model has been applied to many taxa, but this is to our knowledge the first published model for a cnidarian. Future studies might consider estimating parameters for several other species of cnidarians and ctenophores to compare with what has been found for various taxa (Augustine et al., 2011a; Jusup et al., 2010; Saraiva et al., 2011; Mueller et al., 2012; Kooijman, 2013; Pethybridge et al., 2013).

### 5.1. Developmental energetics of *P. noctiluca*

The maximum egg size for *P. noctiluca* is implied by the maternal effect rule and the model predicts a natural variability in egg sizes of about a factor of 14. The occurrence of direct development has been correlated with egg size across Scyphozoa (Berrill, 1949). Only the largest eggs of *A. aurita* undergo direct development for instance. The concept of maturity links up nicely with this observation since there exists a minimum amount of initial energy in the egg for which maturation ceases at birth (Kooijman, 2009). This can be interpreted as the poorest viable eggs which is predicted to be 4 mJ (Table 5). Part of the differences between observed age at birth in Rottini Sandrini and Avian (1983), Avian (1986), and Rosa et al. (2012) might relate to differences in egg size or genotype. Another part may stem from the fact that the transition from planula to ephyra may show some resilience (Avian, 1986).

We computed cumulative energy investment in maturity against age in Fig. 2B and show how much cumulative energy that the individuals from the study by Rottini Sandrini and Avian (1983) invested in  $E_H$  at stages I, II, VI and IX. Our argument that metabolism accelerates right after birth rests upon the assumption that there is no developmental arrest at conception, i.e. no diapause (Kooijman et al., 2011). We ruled out the diapause hypothesis because Avian (1986) did not report a moment when embryo development was stationary; the freshly fertilized oocyte reached the blastula stage in a day at 13.5 °C. If we use the post-metamorphosis/adult values for maximum surface-area assimilation rate and energy conductance we would need to include a 4 d diapause to still fit the observed incubation time; while in reality the embryo already reached the planula stage.

The value of  $\nu$  is well fixed by the available embryo data: timing of developmental stages, temperature dependent incubation times, egg diameter and size at birth (Fig. 2 and Table 4). Another way to test if metabolic acceleration occurs is to see if we can capture adult life history with a much lower  $\{\dot{p}_{Am}\}$  and  $\dot{\nu}$ . We were effectively not able to do this on the basis of the limited information we have so far on ultimate wet mass and reproduction rates. Experimental values of growth at different food levels during the ephyra stage, egg mass and embryo dioxygen consumption will all help confirm or disprove the metabolic acceleration hypothesis.

Metabolic acceleration occurs in many taxa and sometimes it coincides with an important morphological change, but not always

(Kooijman et al., 2011; Kooijman and Lika, accepted for publication; Kooijman, accepted for publication; Lika and Kooijman, accepted for publication). For this particular parameter combination, the organism accelerates its metabolism by a factor of 3 regardless of its prior food history (in other words  $L_j/L_b \approx 3$ ). Metamorphosis is predicted to occur after 6 d at 20 °C,  $f = 1$  at a size of 3.5 mm. It is possible for practical purposes to use post-metamorphosis values for both  $\dot{\nu}$  and  $\{\dot{p}_{Am}\}$  right after birth, because the time it takes to complete metamorphosis is extremely short relative to the time it takes to attain almost the ultimate size at 20 °C,  $f = 1$  (Table 5); this simplifies computations considerably. As soon as more data become available we strongly suggest re-estimating parameter values to check if metamorphosis is really happening so close to birth.

### 5.2. Investment into growth and reproduction

We found low  $f$  values for the three individuals in the laboratory growth experiment by Larson (1987a) (Fig. 5): 0.46, 0.42, 0.45 for individuals A, B and C respectively from that study. Such low  $f$  values are realistic because Larson (1987a) reports that during acclimation many individuals showed shrinking where the mesoglea is degraded first; the four healthiest individuals were used for the growth experiment. During the 14 day growth period, one out of four individuals died (not modeled) and one started to shrink (green squares, Fig. 5). The study further reports that individuals A and B (red circles, green squares Fig. 5) both produced about 40 eggs per day up to day 14. At  $0.4 < f < 0.5$ , the model predicts reproduction rates vastly superior to this number (e.g. Fig. 9B).

The inconsistency is already in the data because the observed reproduction rates (Fig. 3) report that hundreds to thousands of eggs are released in a single spawning event. This large figure was also reported in personal communications with F. Lombard. Scyphozoa in general produce massive amounts of eggs during a spawn (Arai, 1997). We cannot at this stage explain why Larson (1987a) observed only 40 eggs/d except that this may have been a stress induced response.

Recent insight suggests that species which bloom waste resources by increasing somatic maintenance costs in order to decrease maximum size, increase growth rate and reproductive output (Kooijman, 2013). The volume linked somatic maintenance rate costs are much higher than the pseudo-data point but other species might also have high values (e.g. zebrafish, Augustine et al. (2011a)). Most species seem to have a  $\kappa$  value around 0.8 which is not a value that maximizes reproduction rate (Kooijman and Lika, 2014; Lika et al., 2011b). It's extremely interesting that the value of  $\kappa$  found in this study perfectly does.

### 5.3. Importance of reserve for *P. noctiluca*

The high maximum fraction of biomass which is reserve, is a model property which quantifies *P. noctiluca*'s intrinsic adaptation to surviving periods without food. The current parameter set implies that a large part of measured wet mass is reserve, not structure. Since reserves are intuitively associated with lipids this might seem strange for such watery organisms. However, no such assumption is made by DEB theory; reserve comprises rich mixtures of compounds including proteins. Another interesting implied property of the model is the “maximum survival time when starved”  $[E_m]/[\dot{p}_M]$  which is roughly 2.8 months at 20 °C (Table 5). Individuals will actually be able to survive longer than that if it can resorb energy invested into reproduction as well as degrade structure to cover somatic maintenance. As we shall discuss later, *P. noctiluca* most likely does both.

Starvation occurs when  $\kappa \dot{p}_C < [\dot{p}_M] L^3$ . Isotope work (Pecquerie et al., 2010) suggests that structure is degraded continuously (also under non-starvation conditions) and that a substantial fraction of somatic maintenance is used to re-build structure which in the absence of growth is defined as net-synthesis. The re-building of structure is reduced under starvation conditions, which results in shrinking. In this

scenario it is easier to see that shrinking follows naturally due to reduced re-building (causing enrichment of heavy isotopes in structure). Predictions for isotope profiles can and should be tested experimentally to check the realism of this interpretation of shrinking.

Another more easily testable model prediction is that individuals who are starved will continue to reproduce for a ‘while’; the length of that ‘while’ can be formally worked out on the basis of the observed bell diameter and wet mass of an individual using this parameter set (e.g. Fig. 8). Furthermore it might be difficult to detect differences in reproductive output between conditions. An experimenter will be able to clearly disprove these predictions: such a clear deviation between the predicted outcome and reality is stronger in terms of insight than a good fit. On the other hand, if this prediction is in the neighborhood of reality then calculating scenarios beforehand will save time and effort; a month is a long time to follow egg production. The key to future insight is to apply the same experimental protocol for a growth and feeding experiment across different classes of initial sizes. The second key will be to follow individuals. This decreases error when performing mass balancing at that scale.

Future studies wishing to quantify nutrient turnover can do so with the help of the model. The turnover time of compounds in reserve is conditioned by assimilation and mobilization rates. The first depends on food availability (the environment) and the latter on structure. Thus the turnover time of all compounds in reserve is the same and increases with scaled functional response and structure. The residence time of compounds in reserve is  $t_E = E/\dot{p}_C$  and the “maximum reserve residence time”  $t_E = 31$  d (Table 5). The turnover rate of compounds in structure is controlled by somatic maintenance and does not depend on size or food availability.

#### 5.4. On the interpretation of respiration and excretion rates

A really useful feature of DEB theory is that dioxygen consumption as well as ammonia and carbon dioxide production (mineral fluxes) all follow from the dynamics of food, reserve, structure, maturity and reproduction (see Online Appendix A, Section A.2 for details). This means that the nutritional status of the individual will influence predictions for mineral fluxes as we see in Fig. 9C where the model predicts that dioxygen consumption in  $\mu\text{mol/d}$  decreases during starvation as is observed in Malej (1989b).

Dioxygen consumption against length and time are rather close to underlying processes in DEB theory (Fig. 9A–B). Maintenance is linked to  $V$  and assimilation to  $V^{2/3}$  while we assumed that bell diameter is roughly proportional to  $V^{1/3}$ .

If there is no information on the condition and the prior history of an individual then predicting mineral fluxes as a function of biomass and/or mineral flux per unit biomass comes with increasing model assumptions. We already illustrated in Fig. 7A that for a given amount of structure the contribution of reserve to wet biomass varies depending on the food history. We assumed that no starvation occurred and that mass invested into the reproduction buffer did not contribute to total biomass – both of these assumptions might be inexact.

It is theoretically possible to follow growth of several individuals where food level is switched midway starting high then going much lower. If one measures  $\text{O}_2$  consumption regularly for each individual then plots similar to Fig. 9C–F can be made. This would be a very strong set of data both in terms of quantifying the contribution of reserve to wet mass and quantifying the dynamics of reserve mobilization.

Last, the DEB model implies that at puberty all of the energy which previously dissipated as metabolic work involved in maturation gets stored in a reproduction buffer – only a tiny fraction (0.05) of that energy then dissipates in the process of releasing ripe gametes. The grand implication is that at the moment of puberty the mineral fluxes show a decrease (Kooijman, 2010). This particular prediction will be difficult to test, but it should be possible since

the low value of  $\kappa$  exacerbates the predicted jump in mineral fluxes around puberty.

#### 5.5. Flexibility in the timing and size at key life history events

In this study we assumed that both males and females have the same parameters. It seems that males reach the same ultimate length as females which makes this a logical first assumption since ultimate length is  $s_{\infty}/\kappa$  times the ratio of  $\{\dot{p}_{Am}\}$  and  $\{\dot{p}_M\}$ . Paucity in published quantitative data on observed lengths and sizes at sexual maturity and reproductive output under controlled feeding conditions precludes making more detailed assumptions at this stage.

The model predicts that better fed individuals reach puberty faster and at a larger size than less well fed individuals; this is because  $\dot{k}_J < \dot{k}_M$  (Table 5). The inverse would be predicted if  $\dot{k}_J = \dot{k}_M$  and maturity would be reached at the same size if  $\dot{k}_J = \dot{k}_M$  (Kooijman, 2010). The observation that larger *Cyanea* sp. mature earlier than smaller individuals supports this prediction (Brewer (1989) in Arai (1997)). Prior studies on *P. noctiluca* population dynamics assumed that attaining sexual maturity earlier meant at a smaller size (Malej and Malej, 1992). We could not find any empirical support for this.

The model predicts bell diameter at puberty between 2.9 cm ( $f = 0.23$ ) and 5.5 cm ( $f = 1$ ). The prediction is consistent with the observation that females of 4.5 cm and males of 3 cm were considered to be mature in Avian (1986). Rottini Sandrini and Avian (1991) report that gonads are always mature in individuals over 3.5 cm. Franqueville (1971) in Malej and Malej (1992) reports mature females over 6 cm. Mature females under 5 cm bell diameter were never observed and males with mature gonads were  $>4$  cm during 4-year sampling in the field, from 2007 to 2011, at two coastal sites in the straits of Messina (pers. obs. Sara Rosa). If indeed better fed individuals reach puberty faster and at a larger size then this last observation testifies to the good feeding conditions in the straits of Messina.

An individual can theoretically start reproducing anywhere between 21 and 5 months ( $f = 0.23 - 1$ ) at  $13^\circ\text{C}$  and would need an  $f$  a little over 0.5 to do it in 6 months (Fig. 6C). At  $19^\circ\text{C}$  it would theoretically take from 9 to 2 months ( $f = 0.23 - 1$ ) and taking as long as 6 months would indicate a low overall scaled functional response (Fig. 6C). The model predicts that for  $f < 0.14$  growth and maturation cease at puberty (Table 5). The physiological interpretation is that an organism can still mature if ingestion levels are above 14% of the maximum possible for a given size.

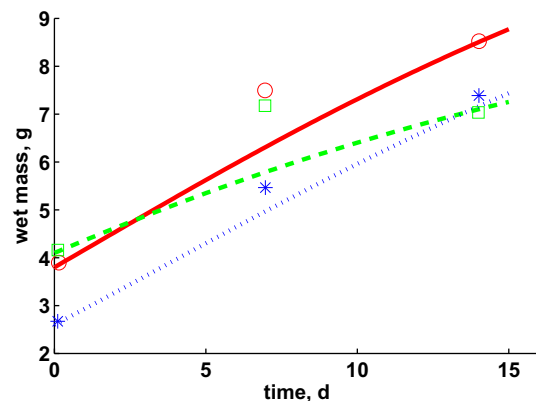


Fig. 5. Wet mass against time. Source: Larson (1987a) ( $28^\circ\text{C}$ ). Red symbol (circle) and red (solid) line corresponds to individual A from that study;  $f = 0.46$ . Green symbol (square) and green (dashed) line corresponds to individual B from that study;  $f = 0.42$ . Blue symbol (star) and blue (dotted) line corresponds to individual C from that study;  $f = 0.45$ . The model predictions assume that the mass of the reproduction buffer does not contribute to the observed wet mass.

**Table 5**

Implied model properties. Compilation of several interesting implied model properties assuming  $f = 1$ , 20 °C and no contribution of mass invested in reproduction to total biomass. Symbols are defined in Table 2. We refer to Table A.2, Online Appendix A, for how these values are computed.

Description	Symbol	Value	Unit
Initial energy in egg	$E_0$	0.06	J
Ash free dry mass of egg		3.0	μg
Fraction of reserve left at birth		0.9	–
Structural length at birth	$L_b$	0.016	cm
Minimum initial energy in egg for which maturation does not cease		0.004	J
Structural length at metamorphosis	$L_j$	0.047	cm
Age at metamorphosis	$a_j$	6	d
Age at 99% of ultimate length		455	d
Ultimate reproduction rate	$\hat{R}_m$	24,690	# d <sup>-1</sup>
Mass at metamorphosis as fraction of maximum mass		$2.2 \cdot 10^{-7}$	–
Mass at puberty as fraction of maximum mass		0.08	–
Fraction of weight that is reserve	$\delta_E$	0.99	–
Functional response for maturation and growth ceasing at puberty		0.14	–
Somatic maintenance rate coefficient	$k_M = [\dot{p}_M]/[E_G]$	0.62	1/d
Maximum structural length	$L_m = \kappa \{ \dot{p}_m \} / [\dot{p}_M]$	0.56	cm
Reserve capacity	$[E_m] = \{ \dot{p}_m \} / \dot{v}$	14.0	kJ/cm <sup>3</sup>
Maximum survival time when starved	$t_{starv} = [E_m] / [\dot{p}_M]$	84	d
Maximum reserve residence time	$t_E$	31	d
Energy density of whole body		20.0	kJ/g (ash free dry mass)
Yield of structure on reserve	$\gamma_{VE}$	0.9	(C-mol V) / (C-mol E)

The reason a minimum  $f$  for which puberty can occur exists in the model is that the organism must pay maturity maintenance costs. It was recently discovered that organisms can be ranked according to a supply–demand spectrum quantified by the supply stress (Lika et al., 2014). The supply stress is a simple function of parameter values and if maturity maintenance would be absent then the supply stress would always be zero. Moreover if maturity maintenance would be zero, all food levels that allow for long term survival would induce reproduction which contradicts a well known stylized fact about animal physiology (Sousa et al., 2008).

We found that the physiological definition of puberty, i.e. stopping allocation to maturity and starting allocation to reproduction to be rather fuzzy but the general consensus in the literature is that gonads must be mature. The terms mature and ripe seem to be used synonymously in the jellyfish literature. We interpret this as being able to produce viable gametes. This has been reported to be less variable for males than for females (Rosa et al., 2012). Perhaps, the reason for this is that females have ripe and unripe gonads and perhaps unripe gonads are mature but do not contain ripe oocytes at the moment they are sampled, as shown in Online Supplementary Figure S.1. Spawning is a continuous event and oocytes are continuously maturing.

## 6. Perspectives: model extensions to account for starvation and spawning/oocyte maturation

The standard DEB model does not cover (species-specific) details around how an organism deals with starvation or how energy invested

into reproduction is converted into eggs (or sperm) and subsequently released into the environment. We think these ‘details’ might be important for future studies as we shall explain below.

First, the extent to which mass invested into reproduction contributes to total biomass remains an open question. The empirical length–wet mass relationship of individuals from the Messina straits (Rosa et al., 2012) suggests that it might be considerable, the reason being that the observed wet mass of a number of organisms exceeds the predicted value for a given length at  $f = 1$  (Fig. 7A).

We are unaware of any published growth curve spanning the early juvenile development till adulthood in controlled laboratory conditions for any Scyphozoa species, let alone *P. noctiluca*. However, length curves reconstructed from the field are typically sigmoid and it is thought this is because of food limitation in the early life stages (Arai, 1997). This further motivates understanding the metabolic handling of starvation over the life-cycle of an individual.

We collected a list of facts which future modules dealing with starvation and reproductive physiology of *P. noctiluca* should respect (Table 6). The first idea resulting from this collection of facts is that reproduction buffer handling rules and starvation rules are probably interconnected since energy invested in reproduction seems to be resorbed during the bleak period.

The second broad idea emanating from Table 6 is that individuals are multiple spawners and oocytes are continuously maturing year round. A spawning event consists of the release of a batch of mature oocytes which are subsequently fertilized and the inter-spawn interval (= speed of oocyte maturation) seems to depend on prior food history

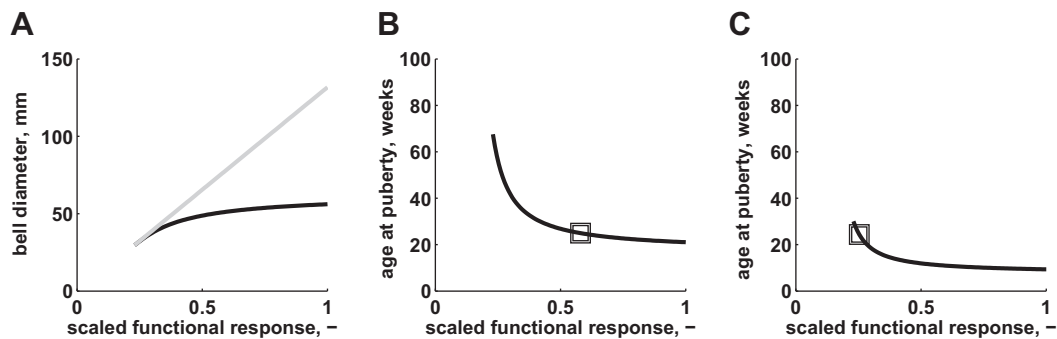


**Fig. 6.** Predicted flexibility in the timing and size at puberty. Length (A) and age (B,C) at puberty as a function of the scaled functional response  $f$ . The model predictions assume  $\delta_{M} = 0.13$ . (A): predicted maximum diameter (gray line) and bell diameter at puberty (black). Water temperature is 13 °C and 19 °C for (B) and (C) respectively. The black squares designate the value of  $f$  for which age at puberty is 6 months at 13 °C (B) and 19 °C (C).

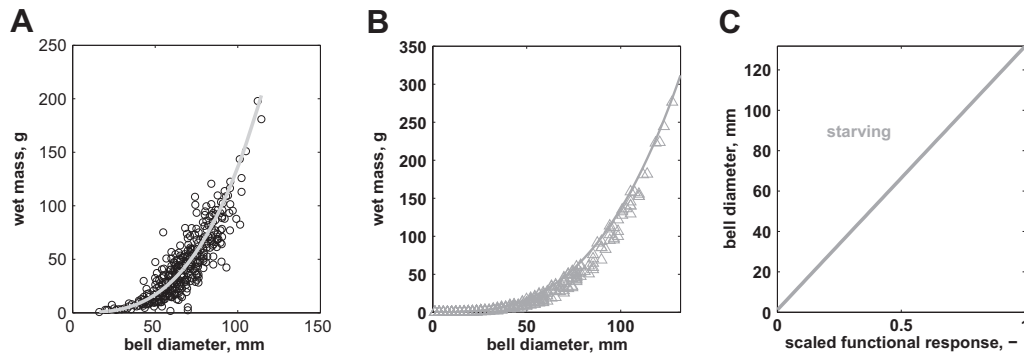


**Fig. 7.** Predicted wet mass against length (A); source (Rosa et al., 2012). Symbols: data; solid gray line: model predictions. The model predictions assume  $f = 1$ ,  $\delta_m = 0.13$  and no contribution from the reproduction buffer. The gray triangles in (B) show the predicted variability in wet mass against bell diameter assuming that reserve density is such that somatic maintenance is covered. The solid line represents predictions for  $f = 1$ . The minimum scaled value of  $f$  for which no starvation occurs at each bell diameter is given in (C) where the solid gray line represents the boundary condition  $[E]/[E_m] = L/L_m/s_m$ , see Tables 1–2.

and temperature. The analysis of future data sets which provide simultaneous length, mass and egg output data for individuals will need to distinguish between the total mass invested into reproduction and mass (# eggs) per spawn.

This line of reasoning invites future work to partition mass/energy invested in reproduction into an unripe and ripe reproduction buffer where the latter compartment comprises ripe gametes ready to be released. This type of extension has already been worked out for three species: anchovy (Pecquerie et al., 2009), oysters (Bernard et al., 2011) and zebrafish (Augustine et al., 2012). Each study varies slightly in species specific details around what stimulates starting and stopping preparation and release of ripe gametes.

Broadly speaking, these studies all assume that if  $\kappa \dot{p}_C < [\dot{p}_M] L^3$  then  $[\dot{p}_M] L^3 - \kappa \dot{p}_C$  should first be taken from the reproduction buffer to complete payment of somatic maintenance costs. When  $[\dot{p}_M] L^3 - \kappa \dot{p}_C > \dot{p}_R$  then part of the structure could be degraded to cover what is missing. The individual dies if its structure shrinks too much. This would be a good starting point for extending the standard DEB model to better understand the metabolic handling of starvation of *P. noctiluca* and capturing

in a simple way how the dynamics of oocyte maturation relates to food and temperature.

## 7. Conclusions

A full life-cycle bioenergetic model for *Pelagia noctiluca* was parameterized to literature data. The overall model fit to data and predictions is consistent with the present day knowledge of the eco-physiology of the species. An exciting and perhaps even uncommon aspect of this study is that detailed knowledge about embryo development was used to infer information on adult metabolism. The DEB model does not distinguish between embryos and adults beyond the fact that the former do not eat and that they allocate to maturity instead of reproduction (Fig. 1). Hence we emphasize that quantifying energy investment in maturation gave insight into energy investment in reproduction for adults. The parameter set we obtain suggests that *P. noctiluca* is highly adapted to survive long periods of starvation since the predicted maximum reserve capacity is extremely high. Moreover we predict that the

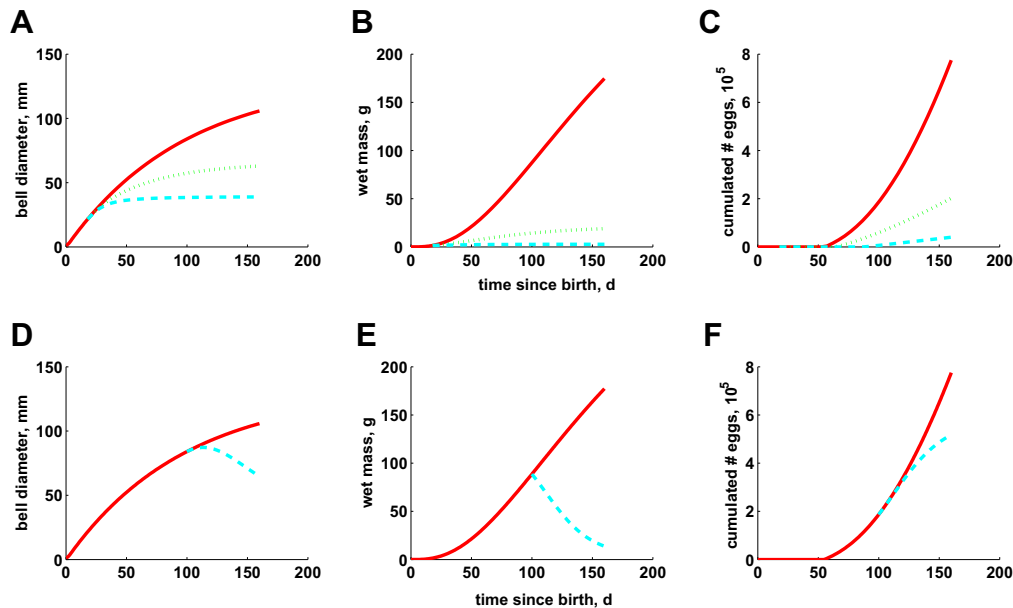


**Fig. 8.** Predicted growth and reproduction at different food levels. Simulations assume 20 °C. In simulations (A–C)  $f = 1$  until 18 days since birth. After that the solid red line denotes length (A), mass (B) and reproductive output (C) at  $f = 1$ . The dotted green line and the dashed cyan line represent those same calculations assuming  $f = 0.5$  and  $f = 0.3$  respectively. The growth in terms of length (E), wet mass (F) and reproductive output (G) are compared for a well fed individual,  $f = 1$  (red solid line) and an individual who was well fed until day 100 and then subsequently put at  $f = 0.3$  (cyan dashed line).

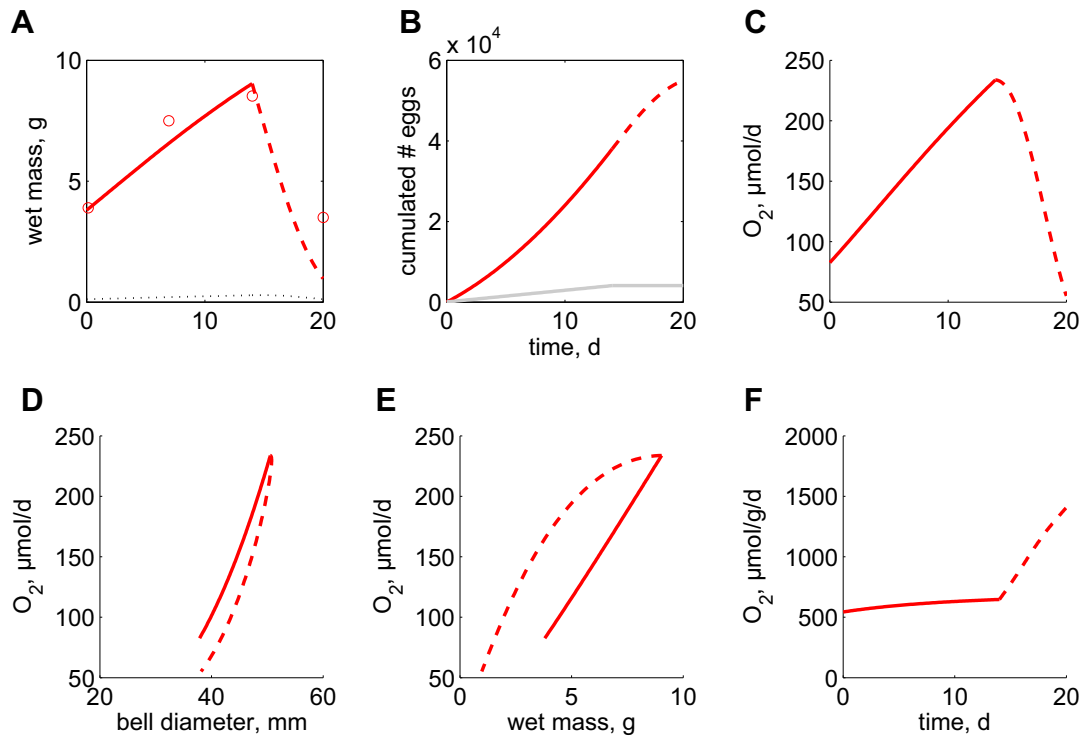


**Fig. 9.** Predicted variability in dioxygen consumption. The model assumes  $\delta_{m, \infty} = 0.13$ ,  $f = 0.46$  (solid line),  $f = 0$  (dashed line) and  $T = 28$  °C. Predicted wet mass (A), reproductive output (B) and dioxygen consumption (C) for individual A during the 14 day feeding followed by 6 day starvation; source: Larson (1987a). Red circle (A) represents data. The black line (A) represents the mass of structure, the red line the combined mass of reserve and of structure. The slope of the gray line (B) corresponds to the 40 eggs/d observed in the study. The predicted dioxygen consumption is then represented in three more ways according to different ways real empirical data are presented: dioxygen consumption against length (D), dioxygen consumption against wet mass (E) and finally mass specific dioxygen consumption (F). The link between the “data” and underlying processes as defined by the DEB model decreases from (D) to (F).

reproductive output of larger individuals is relatively insensitive to changes in food level while wet mass and length are.

Another significant aspect of this study is that an experimenter can now simulate his/her exact protocol before hand and optimize time investment versus information content. We proposed several experiments which would not only test the quantitative predictions we make, but also test the way metabolic organization is conceptualized by DEB theory. This study provides quantitative predictions for dynamic properties of the individual such as the flexible timing and size at maturation and how growth depends on feeding. Such dynamic properties will be useful for making the step to population and ecosystem level modeling frameworks which was the primary motivation for obtaining a first DEB model parameter set.

We propose two main lines of future model development: starvation (energy mobilized is no longer sufficient to cover somatic maintenance), spawning behavior (how many eggs spawned when). We list important empirical facts which such modules should respect and

provide references where detailed formulations of the modules are found. Adding or removing the modules is simple and amounts to stepping up or down in the level of physiological detail of the model. Simple translation rules between levels of biological detail are essential when aiming to couple individual models to population models.

#### Acknowledgments

This study was supported by post-doctoral research grant Jellywatch funded by the Provence Alpes Côtés d’Azur Region and the FEDER Program (Contract # 2009 - 21541–34380). Part of the research of SA, JCP and FC has been supported by the project “MODIMIG” (EC2CO, France). SA received additional support from the Van Coeverden Adriani Foundation. The authors thank Fabien Lombard for helpful discussions on the reproduction and behavior of *P. noctiluca*. The authors extend thanks to all of the participants of the DEB course 2013 for stimulating DEB theory discussions. Finally, the comments of Elke Zimmer and

**Table 6**

Compilation of qualitative facts pertaining to both reproduction and starvation. Several general observations on physiological response of organisms to starvation and details around reproduction are collected in this table. These qualitative facts should be taken into account when formulating starvation and spawning rules.

Organisms do not shrink isomorphically: before starvation individuals are dome shaped, oral arms are expanded and after starvation the umbrella is flattened and depressed on both sides, oral arms are contracted	Malej (1991)
When individuals are starved metabolic rates slow down	Malej (1991)
During starvation the reduction in $\text{NH}_3$ excretion is more pronounced than the reduction in $\text{O}_2$ consumption which results in lower O:N ratio in starving animals	Malej (1991)
Oocytes in every stage of maturation are present in gonads all year round	Rottini Sandrini and Avian (1991)
During spawning all mature oocytes are released via a mucus ribbon	Rottini Sandrini and Avian (1991)
Spawning is continuous; after spawning a female may spawn again after 1–2 d (19–21 °C) or 7 d ( $\leq 16$ °C) depending on the temperature	Avian and Rottini Sandrini (1991)
Food affects speed of oocyte maturation	Rottini Sandrini and Avian (1991)
During low food availability autolytic effects on ovaries were observed	Rottini Sandrini and Avian (1991)
Very large females can show empty discolored gonads	Sara Rosa (pers. obs.)

that of 2 anonymous reviewers considerably improved the quality of the manuscript.

## Appendix A. Supplementary data

Supplementary data to this article can be found online at <http://dx.doi.org/10.1016/j.seares.2014.06.007>.

## References

- Arai, M.N., 1997. *A Functional Biology of Scyphozoa*. Chapman & Hall, London.
- Augustine, S., Gagnaire, B., Adam-Guillermin, C., Kooijman, S.A.L.M., 2011a. Developmental energetics of zebrafish, *Danio rerio*. *Comp. Biochem. Physiol. A* 159, 275–283.
- Augustine, S., Litvak, M.K., Kooijman, S.A.L.M., 2011b. Stochastic feeding of teleost fish and their metabolic handling of starvation. *J. Sea Res.* 66, 411–418.
- Augustine, S., Gagnaire, B., Adam-Guillermin, C., Kooijman, S.A.L.M., 2012. Effects of uranium on the metabolism of zebrafish, *Danio rerio*. *Aquat. Toxicol.* 118–119, 9–26.
- Avian, M., 1986. Temperature influence on in vitro reproduction and development of *Pelagia noctiluca* (Forskål). *Boll. Zool.* 53 (4), 385–391.
- Avian, M., Rottini Sandrini, L., 1991. Oocyte development in four species of scyphomedusa in the northern Adriatic Sea. *Hydrobiologia* 216 (217), 189–195.
- Bernard, L., de Kermoyan, G., Pouvreau, S., 2011. Effect of phytoplankton and temperature on the reproduction of the Pacific oyster *Crassostrea gigas*: investigation through DEB theory. *J. Sea Res.* 66 (4), 349–360.
- Berrill, N.J., 1949. Developmental analysis of scyphomedusae. *Biol. Rev.* 24, 393–410.
- CIESM, 2001. Gelatinous zooplankton outbreaks: theory and practice. CIESM Workshop Series, n. 14 (112 pages, Monaco. URL <http://www.ciesm.org/online/monographs/Naples.pdf>).
- Daly Yahia, M.N., Goy, J., Daly Yahia-Kéfi, O., 2003. Distribution et écologie des Méduses (Cnidaria) du golfe de Tunis (Méditerranée sud occidentale). *Oceanol. Acta* 26 (5–6), 645–655 (URL <http://www.sciencedirect.com/science/article/pii/S0399178403000719>).
- Ferraris, M., Berline, L., Lombard, F., Guidi, L., Elineau, A., Mendoza-Vera, J.M., Lilley, M.K.S., Taillandier, V., Gorsky, G., 2012. Distribution of *Pelagia noctiluca* (Cnidaria, Scyphozoa) in the Ligurian Sea (NW Mediterranean Sea). *J. Plankton Res.* 34 (10), 874–885.
- Goy, J., Morand, P., Etienne, M., 1989. Long-term fluctuations of *Pelagia noctiluca* (Cnidaria, Scyphomedusa) in the western Mediterranean Sea. Prediction by climatic variables. *Deep-Sea Res.* 36 (2), 269–279.
- Hamner, W.N., Janssen, R.M., 1974. Growth, degrowth, and irreversible cell differentiation in *Aurelia aurita*. *Am. Zool.* 14, 833–849.
- Jusup, M., Klanjšček, T., Matsuda, H., Kooijman, S.A.L.M., 2010. A full lifecycle bioenergetic model for bluefin tuna. *PLoS ONE* 6 (7), e21903.
- Kakinuma, Y., 1975. An experimental study of the life cycle and organ differentiation of *Aurelia aurita* Lamarck. *Bull. Marine Biol. Station Asamushi* 15 (3–6), 101–113.
- Kogošek, T., Bogunović, B., Malej, A., 2010. Recurrence of bloom-forming scyphomedusae: wavelet analysis of a 200-year time series. *Hydrobiologia* 645, 81–96.
- Kooijman, S.A.L.M., 2009. What the egg can tell us about its hen: embryonic development on the basis of dynamic energy budgets. *J. Math. Biol.* 58 (3), 377–394.
- Kooijman, S.A.L.M., 2010. *Dynamic Energy Budget Theory for metabolic organization* (Cambridge).
- Kooijman, S.A.L.M., 2013. Waste to hurry: dynamic energy budgets explain the need of wasting to fully exploit blooming resources. *Oikos* 122, 348–357. <http://dx.doi.org/10.1111/j.1600-0706.2012.00098.x>.
- Kooijman, S.A.L.M., 2014. Metabolic acceleration in animal ontogeny: an evolutionary perspective. *J. Sea Res.* 94, 128–137.
- Kooijman, S.A.L.M., Lika, K., 2014b. Resource allocation to reproduction in animals. *Biol. Rev.* <http://dx.doi.org/10.1111/brv.12082/full> (000–000).
- Kooijman, S.A.L.M., Lika, K., 2014. Comparative energetics of the 5 fish classes on the basis of Dynamic Energy Budgets. *J. Sea Res.* 94, 19–28.
- Kooijman, S.A.L.M., Sousa, T., Pecquerie, L., Van der Meer, J., Jager, T., 2008. From food-dependent statistics to metabolic parameters, a practical guide to the use of dynamic energy budget theory. *Biol. Rev.* 83 (4), 533–552.
- Kooijman, S.A.L.M., Pecquerie, L., Augustine, S., Jusup, M., 2011. Scenarios for acceleration in fish development and the role of metamorphosis. *J. Sea Res.* 66, 419–423.
- Larson, R.J., 1987a. A note on the feeding, growth and reproduction of the epipelagic scyphomedusa *Pelagia noctiluca* (Forskål). *Biol. Oceanogr.* 4 (4), 447–454.
- Larson, R.J., 1987b. Respiration and carbon turnover rates of medusae from the NE Pacific. *Comp. Biochem. Physiol. A* 87 (1), 93–100.
- Lika, K., Kooijman, S.A.L.M., 2014. Metabolic acceleration in Mediterranean Perciformes. *J. Sea Res.* 94, 37–46.
- Lika, K., Kearney, M.R., Freitas, V., van der Veer, H.W., van der Meer, J., Wijsman, J.W.M., Pecquerie, L., Kooijman, S.A.L.M., 2011a. The “covariation method” for estimating the parameters of the standard Dynamic Energy Budget model I: philosophy and approach. *J. Sea Res.* 66, 270–277.
- Lika, K., Kearney, M.R., Kooijman, S.A.L.M., 2011b. The “covariation method” for estimating the parameters of the standard Dynamic Energy Budget model II: properties and preliminary patterns. *J. Sea Res.* 66, 278–288.
- Lika, K., Augustine, S., Pecquerie, L., Kooijman, S.A.L.M., 2014. The bijection from data to parameter space with the standard DEB model quantifies the supply–demand spectrum. *J. Theor. Biol.* <http://dx.doi.org/10.1016/j.jtbi.2014.03.025>.
- Malej, A., 1989a. Behaviour and trophic ecology of the jellyfish *Pelagia noctiluca*. *J. Exp. Mar. Biol. Ecol.* 126, 259–270.
- Malej, A., 1989b. Respiration and excretion rates of *Pelagia noctiluca* (Semaestomeae, Scyphozoa). Proceedings of the 21st EMBS. Academy of Sciences – Institute of Oceanology, Gdańsk, pp. 107–113 (14–19 September).
- Malej, A., 1991. Rates of metabolism of jellyfish as related to body weight, chemical composition and temperature. Jellyfish Blooms in the Mediterranean. Proceedings of the II Workshop on Jellyfish in the Mediterranean Sea. No. 47 in MAP Technical Reports. UNEP, Athens, pp. 253–259.
- Malej, A., Malej, M., 1992. Population dynamics of the jellyfish *Pelagia noctiluca* (Forskål 1775). In: Colombo, Giuseppe, et al. (Eds.), Marine eutrophication and population dynamics. Proceedings of the 25th EMBS. Olsen & Olsen, Fredensborg, Denmark, pp. 215–219.
- Malej, A., Malej, A.J., 2004. Invasion of the jellyfish *Pelagia noctiluca* in the Northern Adriatic: a non success story. H. Humont et al., pp. 273–285.
- Malej, A., Faganelli, J., Pezdič, J., 1993. Stable isotope and biochemical fractionation in the marine pelagic food chain: the jellyfish *Pelagia noctiluca* and net zooplankton. *Mar. Biol.* 116, 565–570.
- Mariottini, G.L., Giacco, E., Pane, L., 2008. The mauve stinger *Pelagia noctiluca* (Forskål, 1775). Distribution, ecology, toxicity and epidemiology of stings. A review. *Mar. Drugs* 6, 496–513.
- Morand, P., Carré, C., Biggs, D.C., 1987. Feeding and metabolism of the jellyfish *Pelagia noctiluca* (Scyphomedusae, Semaestomeae). *J. Plankton Res.* 9 (4), 651–665.
- Mueller, C., Augustine, S., Kearney, M.R., Kooijman, S.A.L.M., Seymour, R., 2012. The trade-off between maturation and growth during accelerated development in frogs. *Comp. Biochem. Physiol. A* 163, 95–102.
- Pecquerie, L., Pettigat, P., Kooijman, S.A.L.M., 2009. Modeling fish growth and reproduction in the context of the dynamic energy budget theory to predict environmental impact on anchovy spawning duration. *J. Sea Res.* 62, 93–105.
- Pecquerie, L., Nisbet, R.M., Fablet, R., Lorrain, A., Kooijman, S.A.L.M., 2010. The impact of metabolism on stable isotope dynamics: a theoretical framework. *Philos. Trans. R. Soc. B* 365, 3455–3468.
- Pethybridge, H., Roos, D., Loizeau, V., Pecquerie, L., Bacher, C., 2013. Responses of European anchovy vital rates and population growth to environmental fluctuations: an individual-based modeling approach. *Ecol. Model.* 250, 370–383 (URL <http://www.sciencedirect.com/science/article/pii/S0304380012005558>).
- Piraino, S., Boero, F., Aeschbach, B., Schmid, V., 1996. Reversing the life cycle: medusae transforming into polyps and cell transdifferentiation in *Turritopsis nutricula* (Cnidaria, Hydrozoa). *Biol. Bull.* 90 (3), 302–312.
- Rosa, S., Pansera, M., Granata, A., Guglielmo, L., 2012. Interannual variability, growth, reproduction and feeding of *Pelagia noctiluca* (Cnidaria: Scyphozoa) in the Straits of Messina (Central Mediterranean Sea): linkages with temperature and diet. *J. Mar. Syst.* 111–112, 97–107 (URL <http://www.sciencedirect.com/science/article/pii/S0924796312001972>).
- Rottini Sandrini, L., Avian, M., 1983. Biological cycle of *Pelagia noctiluca*: morphological aspects of the development from planula to ephyra. *Mar. Biol.* 74, 169–174.
- Rottini Sandrini, L., Avian, M., 1991. Reproduction of *Pelagia noctiluca* in the central and northern Adriatic Sea. *Hydrobiologia* 216 (217), 197–202.
- Saraiva, S., van der Meer, J., Kooijman, S.A.L.M., Sousa, T., 2011. DEB parameters estimation for *Mytilus edulis*. *J. Sea Res.* 66 (4), 289–296 (URL <http://www.sciencedirect.com/science/article/pii/S1385110111000931>).
- Sousa, T., Domingos, T., Kooijman, S.A.L.M., 2008. From empirical patterns to theory: a formal metabolic theory of life. *Philos. Trans. R. Soc. B* 363, 2453–2464.
- Sousa, T., Domingos, T., Poggiale, J.C., Kooijman, S.A.L.M., 2010. Dynamic energy budget restores coherence in biology. *Philos. Trans. R. Soc. B* 365, 3413–3428.